Hill, T.L., Neild, S.A., Cammarano, A. and Barton, D.A.W. (2017) The Significance of Nonlinear Normal Modes for Forced Responses. In: Proceedings of the 35th IMAC, A Conference and Exposition on Structural Dynamics 2017, Garden Grove, CA, USA, 30 Jan - 02 Feb 2017, pp. 135-142. ISBN 9783319455038.

The significance of nonlinear normal modes for forced responses

T.L. Hill[1] *, S.A. Neild[1], A. Cammarano[2] and D.A.W. Barton[3]

[1] Department of Mechanical Engineering, University of Bristol, Bristol, UK, BS8 1TR

[2] School of Engineering, University of Glasgow, Glasgow, UK, G12 8QQ

[3] Department of Engineering Mathematics, University of Bristol, Bristol, UK, BS8 1TR

ABSTRACT

Nonlinear normal modes (NNMs) describe the unforced and undamped periodic responses of nonlinear systems. NNMs have proven to be a valuable tool, and are widely used, for understanding the underlying behaviour of nonlinear systems. They provide insight into the types of behaviour that may be observed when a system is subjected to forcing and damping, which is ultimately of primary concern in many engineering applications.

The definition of an NNM has seen a number of evolutions, and the contemporary definition encompasses all periodic responses of a conservative system. Such a broad definition is essential, as it allows for the wide variety of responses that nonlinear systems may exhibit. However, it may also lead to misleading results, as some of the NNMs of a system may represent behaviour that will only be observed under very specific forcing conditions, which may not be realisable in any practical scenario. In this paper, we investigate how the significance of NNMs may differ and how this significance may be quantified. This is achieved using an energy-based method, and is validated using numerical simulations.

Keywords: Nonlinear normal modes, Nonlinear structural dynamics, Backbone curves, Energy balancing, Nonlinear beam

Introduction

Nonlinear normal modes (NNMs) are an established tool for understanding nonlinear dynamic systems. NNMs describe the dynamic behaviour of an unforced and undamped system, but may be used to interpret the underlying behaviour of the forced and damped responses [1, 2]. This simplifies the process of analysing the forced responses, particularly complex features such as isolas [3, 4, 5].

The first definition of an NNM was proposed by Rosenberg as any *vibration-in-unison* of the underlying conservative system [6, 7]. Since this original definition, the theory of NNMs has seen two major extensions. Firstly, NNM theory has been extended to include the damped dynamics. This extension was led by Shaw and Pierre [8, 9], and more has received more recent attention from Haller and Ponsioen [10]. Secondly, the definition of a conservative NNM has been expanded to encompass a greater variety of behaviours. It is the second of these extensions, relating to the conservative dynamics, which is of interest in this paper.

The contemporary definition of an NNM includes any *nonnecessarily synchronous periodic motion* [1]. This allows the inclusion of motions that are not in-unison, such as out-of-unison motion [11], but which exhibit the useful same properties as NNMs. However, it has been observed that not all NNMs appear to relate to the forced responses [12]. As such, the objective of this paper is to investigate the relationship between the forced responses and NNMs, in order to understand why some NNMs appear to have little influence on the forced response.

*Address all correspondence to this author - tom.hill@bristol.ac.uk.

This paper begins by introducing a pinned-pinned beam with a torsional spring at one end. A model for this beam, consisting of two linear modes[1], is derived using a Galerkin method, and nonlinear terms arise from the dynamic tension in the beam. A numerical continuation technique is then used to find a series of NNM branches, demonstrating the complexity that may arise from a relatively simple nonlinear system. The abundance of NNMs makes it difficult to reliably interpret the forced responses. However, an understanding of which NNMs relate to the forced responses, and which do not, would allow some NNM branches to be neglected, thus simplifying the interpretation.

To gain an understanding of this relationship, an energy-based technique, previously discussed in [13], is then used to find the damping levels that are required to observe the NNMs in the forced responses, given a specific forcing. This reveals that some NNMs require an extremely low level of damping to be observed – much lower than is typically seen in engineering structures. This explains why such responses are not often seen. Finally, to demonstrate that these seldom-observed NNMs may, in extreme cases, exist in forced responses, a case with very low damping is considered, and a forced response is computed.

Nonlinear normal modes of an example system

A nonlinear beam example

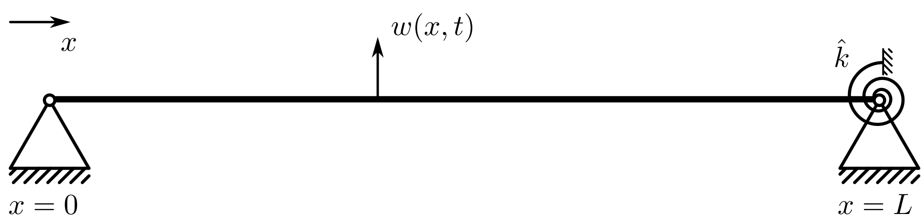

Fig. 1 A schematic of the pinned-pinned beam considered throughout this paper.

To motivate discussion throughout this paper, the nonlinear beam, depicted in Fig. 1, is considered. This beam is pinned at both ends and has a torsional spring at $x = L$, where x is the distance along the beam and L is the length of the beam. This spring is linear, with the stiffness constant $\hat{k}$.

As described in [14, 15], the unforced and undamped vertical deflection of the beam is governed by the expression

$$\rho\hat{A}\frac{\partial^2 w(x,t)}{\partial t^2}+EI\frac{\partial^4 w(x,t)}{\partial x^4}-\left[\frac{E\hat{A}}{2L}\int_0^L\left(\frac{\partial w(x,t)}{\partial x}\right)^2\mathrm{d}x\right]\frac{\partial^2 w(x,t)}{\partial x^2}+\delta\left(x-L\right)\hat{k}\psi(L,t)=0\,, \tag{1}$$

where w, δ and $\psi(x,t)$ denote the vertical displacement of the beam, the Dirac delta function and the rotation of the beam respectively. The density, cross-sectional area, Young's modulus and second moment of area are described by the constants ρ, $\hat{A}$, E and I respectively. The nonlinearity in this system arises from the dynamic tension in the beam – represented by the terms in the square bracket in Eq. (1).

The dynamics of interest for this paper may be captured by considering the first two underlying linear modes, such that the vertical deflection may be written

$$w(x,t)=\theta_1(x)q_1(t)+\theta_2(x)q_2(t)\,, \tag{2}$$

where θ_i represents the i^{th} linear modeshape and q_i represents the displacement of the i^{th} linear mode. As described in [15], θ_i may be computed using

$$\theta_i(x)=\sqrt{2}\left[1-2\frac{EI}{\hat{k}L}\sin^2(\beta_i)-\left(\frac{\sin(\beta_i)}{\sinh(\beta_i)}\right)^2\right]^{-\frac{1}{2}}\left[\sin\left(\frac{\beta_i}{L}x\right)-\frac{\sin(\beta_i)}{\sinh(\beta_i)}\sinh\left(\frac{\beta_i}{L}x\right)\right], \tag{3}$$

[1]Throughout this paper, the term *mode* is used to refer to an underlying linear mode of the system. An NNM is a separate concept, and is typically composed of a combination of linear modes.

where β_i is found by solving

$$\cot(\beta_i) - \coth(\beta_i) + 2EI\frac{\beta_i}{\hat{k}L} = 0\,. \tag{4}$$

To find the modal equation of motion, Galerkin's method is applied to Eq. (1), as detailed in [15]. This leads to the expression

$$\ddot{\mathbf{q}} + \mathbf{\Lambda}\mathbf{q} + \mathbf{N}_q\left(\mathbf{q}\right) = 0\,, \tag{5}$$

where $\mathbf{q}$, $\mathbf{\Lambda}$ and $\mathbf{N}_q$ denote the vector of modal displacements, the matrix of linear natural frequencies and the vector of nonlinear terms, which are written

$$\mathbf{q} = \begin{pmatrix} q_1 \\ q_2 \end{pmatrix}, \quad \mathbf{\Lambda} = \begin{bmatrix} \omega_{n1}^2 & 0 \\ 0 & \omega_{n2}^2 \end{bmatrix}, \quad \mathbf{N}_q = \begin{pmatrix} \alpha_1 q_1^3 + 3\alpha_2 q_1^2 q_2 + \alpha_3 q_1 q_2^2 + \alpha_4 q_2^3 \\ \alpha_2 q_1^3 + \alpha_3 q_1^2 q_2 + 3\alpha_4 q_1 q_2^2 + \alpha_5 q_2^3 \end{pmatrix}, \tag{6}$$

where ω_{ni} is the linear natural frequency of the i^{th} mode and where α_k are nonlinear coefficients. The linear natural frequencies are found using the expression

$$\omega_{ni}^2 = \frac{EI}{\rho\hat{A}}\left(\frac{\beta_i}{L}\right)^4, \tag{7}$$

and the nonlinear coefficients are found from

$$\begin{aligned}
\alpha_1 &= \frac{-E}{2L^2\rho}\left[\int_0^L \theta_1'\theta_1'\mathrm{d}x\right]\left[\int_0^L \theta_1''\theta_1\mathrm{d}x\right], \qquad \alpha_2 = \frac{-E}{2L^2\rho}\left[\int_0^L \theta_1'\theta_1'\mathrm{d}x\right]\left[\int_0^L \theta_1''\theta_2\mathrm{d}x\right], \\
\alpha_3 &= \frac{-E}{2L^2\rho}\left\{2\left[\int_0^L \theta_1'\theta_2'\mathrm{d}x\right]\left[\int_0^L \theta_2''\theta_1\mathrm{d}x\right] + \left[\int_0^L \theta_2'\theta_2'\mathrm{d}x\right]\left[\int_0^L \theta_1''\theta_1\mathrm{d}x\right]\right\}, \\
\alpha_4 &= \frac{-E}{2L^2\rho}\left[\int_0^L \theta_2'\theta_2'\mathrm{d}x\right]\left[\int_0^L \theta_2''\theta_1\mathrm{d}x\right], \qquad \alpha_5 = \frac{-E}{2L^2\rho}\left[\int_0^L \theta_2'\theta_2'\mathrm{d}x\right]\left[\int_0^L \theta_2''\theta_2\mathrm{d}x\right].
\end{aligned} \tag{8}$$

The physical parameters chosen for this paper are listed in Table 1.

Table 1 The physical parameters of the beam.

Length (L)	Depth (d)	Height (h)	Density (ρ)	Young's Modulus (E)	Torsional stiffness ($\hat{k}$)
500 mm	30 mm	1 mm	7800 kg m^{-3}	2×10^{11} N m^{-2}	10 N m rad^{-1}

Using Eqs. (7) and (8), these physical parameters give the linear natural frequencies and nonlinear parameters shown in Table 2.

Table 2 The linear natural frequencies, ω_{ni}, and nonlinear parameters, α_k, of the beam.

ω_{n1} [rad s^{-1}]	ω_{n2}	α_1 ($\times 10^{10}$)	α_2	α_3	α_4	α_5
125.91	418.41	8.81	-1.31	34.70	-5.12	133.63

Nonlinear normal modes of the beam model

The contemporary definition of an NNM encompasses any periodic motion of the underlying unforced and undamped system [1]. Numerous analytical and numerical methods may be used to compute the NNMs of a system [16, 17], but here the numerical continuation software AUTO-07p is employed [18].

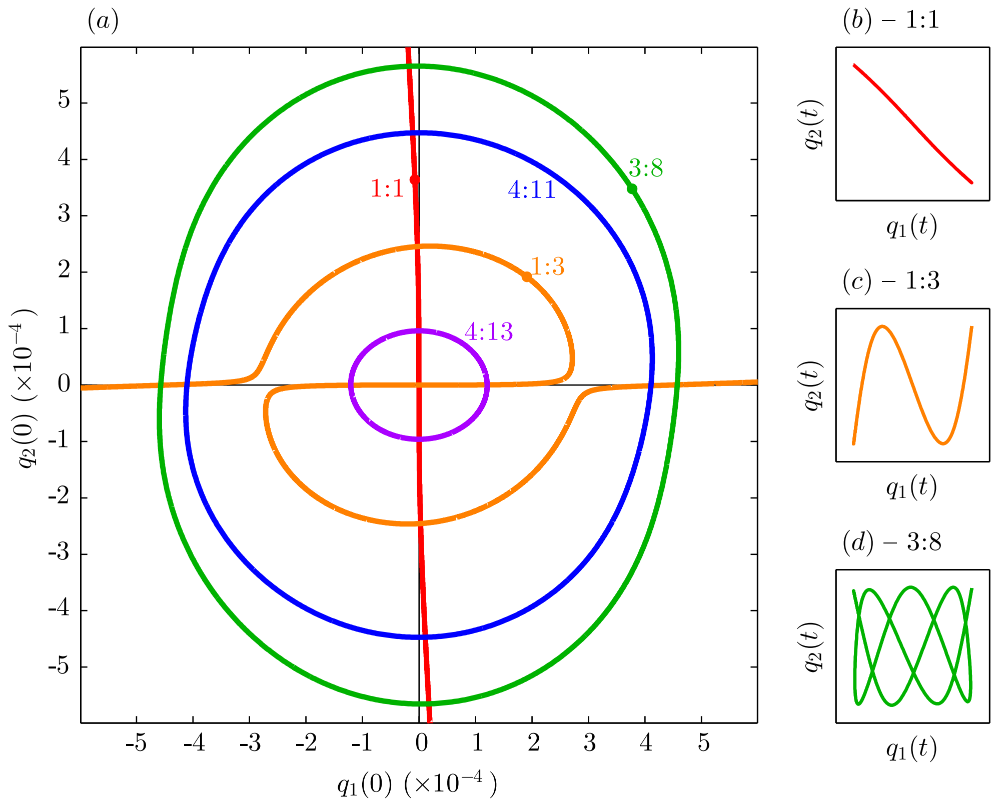

Fig. 2 Panel (a) shows five NNM branches (i.e. the loci of NNMs) of the nonlinear beam model, in the projection of the initial displacements of the two modes. The branch labels denote the ratio between the fundamental frequencies of the two modes. A dot on the 1:1, 1:3 and 3:8 branches mark the positions of the NNMs that are shown, parameterised in time, in panels (b), (c) and (d) respectively. These panels are in the projection of the first modal displacement, $q_1(t)$, against the second modal displacement, $q_2(t)$.

Figure 2(a) shows five of the NNM branches of the two-mode model of the example system. These are represented in the projection of the initial displacement of the first mode, $q_1(0)$, against that of the second mode, $q_2(0)$. The initial modal velocities are both zero, i.e. $\dot{q}_1(0) = \dot{q}_2(0) = 0$. These NNM branches represent the loci of periodic solutions to Eq. (5). The NNM branches are colour-coded and labelled according to the ratio between the fundamental frequencies of the two modes, where the fundamental frequency is defined as the frequency of the highest-amplitude Fourier coefficient of the response. For example, considering a response on the 3:8 branch, the fundamental component of the first mode oscillates three times per period, whilst the fundamental component of the second mode oscillates eight times per period. This may also be described by defining the *base frequency* as $\omega = 2\pi/T$, where T is the period of the response, and the fundamental response frequency of the i^{th} mode as ω_{ri}. For a branch labelled $n : m$, the fundamental response frequencies are $\omega_{r1} = n\omega$ and $\omega_{r2} = m\omega$. This is demonstrated in Figs. 2(b), 2(c) and 2(d), which show the time-parameterised responses of NNMs from the 1:1, 1:3 and 3:8 branches respectively. The positions of these NNMs are marked with dots in Fig. 2(a).

Whilst the model of the beam is approximate (due to assumptions made in the derivation of the equations of motion, and the assumption that the higher modes are negligible) the numerical solutions for this model are accurate to within the tolerances of the numerical method. As such, the NNM branches shown in Fig. 2 appear to be a genuine feature of the dynamics of the model. This demonstrates the complexity that may arise from a relatively simple nonlinear model. Furthermore, a huge number of additional NNM branches may be found if higher ratios between the fundamental frequencies are considered (i.e. higher than 4:13), or if responses with initial conditions beyond those shown in Fig. 2 are used.

The large number of NNM branches presents a problem: as NNMs are often used to interpret the responses of a system when subjected to forcing and damping, the abundance of NNM branches indicates that the forced responses must exhibit an extremely diverse range of dynamic behaviours. However, as such behaviour is not typically observed in the forced responses, it is clear that not all NNM branches correspond to the forced responses. As such, in the following section, we investigate the relationship between the NNMs and forced responses. This will provide insight into why the dynamic behaviour described by some NNMs are observed in the forced responses, and some are not.

Relating nonlinear normal modes to forced responses

A method for relating NNMs and forced responses was introduced in [19] and further developed in [13]. This method relies on the argument that, for any steady-state periodic response, the net energy gained by the system due to forcing must equal the net energy dissipated by the damping. As such, if it is assumed that a forced system may exhibit a response that is identical to an NNM response, the forcing and damping must be such that this energy criterion is satisfied. In this section, we assume that the forcing is known and we use the energy criterion to find the damping that is required for the forced response to match that of a particular NNM (i.e. to reach resonance at that point on the NNM branch).

For a two-mode system, the energy criterion may be written

$$E_{f1} + E_{f2} = E_{d1} + E_{d2}\,, \tag{9}$$

where E_{fi} is the net energy gained by the i^{th} mode due to external forcing, and E_{di} represents the net energy dissipated by the i^{th} mode via damping. These are computed using

$$E_{fi} = \int_0^T f_i(t)\dot{q}_i(t)\mathrm{d}t\,, \qquad E_{di} = \int_0^T d_i(t)\dot{q}_i(t)\mathrm{d}t\,, \tag{10}$$

where f_i and d_i denote the forcing and damping applied to the i^{th} linear mode respectively.

For this example, we consider the case where the first mode is sinusoidally forced and both modes have proportional linear damping such that

$$f_1 = F\sin(\omega t)\,, \qquad f_2 = 0\,, \qquad d_1 = 2\zeta\omega_{n1}\dot{q}_1\,, \qquad d_2 = 2\zeta\omega_{n2}\dot{q}_2\,, \tag{11}$$

where F represents the forcing amplitude, ω is the base frequency (defined as $\omega = 2\pi/T$) and where ζ is the linear damping ratio. Substituting Eqs. (10) and (11) into Eq. (9) leads to

$$\int_0^T F\sin(\omega t)\,\dot{q}_1(t)\mathrm{d}t = \int_0^T 2\zeta\omega_{n1}\dot{q}_1^2\mathrm{d}t + \int_0^T 2\zeta\omega_{n2}\dot{q}_2^2\mathrm{d}t\,, \tag{12}$$

which may then be rearranged to give an expression for the damping ratio, written

$$\zeta = \frac{F\int_0^T \sin(\omega t)\,\dot{q}_1(t)\mathrm{d}t}{2\left(\omega_{n1}\int_0^T \dot{q}_1^2\mathrm{d}t + \omega_{n2}\int_0^T \dot{q}_2^2\mathrm{d}t\right)}\,. \tag{13}$$

Using numerical solutions for the NNMs, the integrals in Eq. (13) may be computed. This gives the damping ratio, ζ, that is required for the forced response to reach resonance at each NNM.

Figure 3 shows five NNM branches for the beam model, as previously shown in Fig. 2, along with a colour-scheme depicting the damping ratio required to achieve resonance at each point (i.e. at each NNM). As previously, the branches are labelled according to the ratio between the fundamental frequencies of the modes. The amplitude of the sinusoidal forcing applied to the first linear mode is $F = 0.1$.

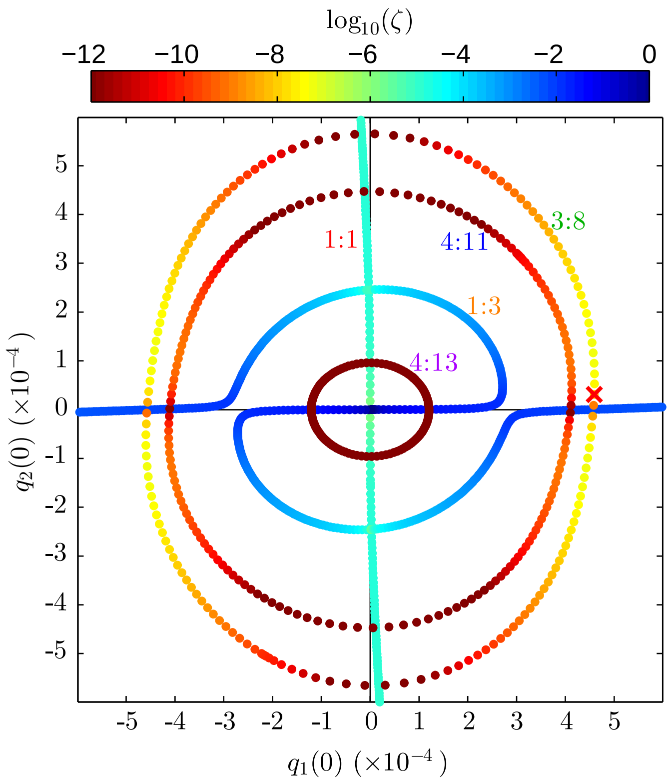

Fig. 3 Five NNM branches of the nonlinear beam model shown in the projection of the initial displacements of the two modes. A colour-scheme is used to show the damping ratio, ζ, that is required for a forced response to resonate at each point on the branch when the forcing amplitude is $F = 0.1$. The red cross marks an NNM on the 3:8 branch where the required damping ratio is $\zeta = 10^{-8}$. This point is used to investigate a forced response in the following section.

It can be seen that the 1:1 branch requires a fairly low damping. This is due to the small contribution of the first mode to the 1:1 responses, compared to the second mode. As only the first mode is forced, little energy in transferred into the system, whilst the high-amplitude second mode causes a large amount of energy-loss via damping. As such, the damping ratio must be low to achieve resonance on this branch. The 1:3 branch is dominated by the first linear mode for the majority of NNMs. As such, the damping is of the order that is typically seen in engineering structures. However, the 3:8 branch requires an extremely low level of damping – much lower than is seen in typical engineering structures – and the required damping for the 4:11 and 4:13 branches is lower still. This suggests a difference between the NNM branches with *low* frequency ratios (i.e. the 1:1 and 1:3 branches) and those with higher ratios (i.e. the 3:8, 4:11 and 4:13 branches). Namely, it appears that the forced responses only resonate with high-ratio NNMs when the damping is extremely low.

Forced responses

We now consider a set of forced responses for the nonlinear beam model. As in the previous section, the system has proportional linear modal damping, and a sinusoidal force with amplitude $F = 0.1$ is applied to the first linear mode. A red cross in Fig. 3 marks a response on the 3:8 branch where the required damping ratio is $\zeta = 10^{-8}$. This damping ratio is used to find the forced response, and the NNM response at this point is used as an initial orbit from which to start the continuation, using AUTO-07p.

Figure 4(a) shows the NNM branches, as given in previous figures, along with a set of forced responses of the system. It can be seen that the forced responses are enveloping the 3:8 branch and an inset panel is

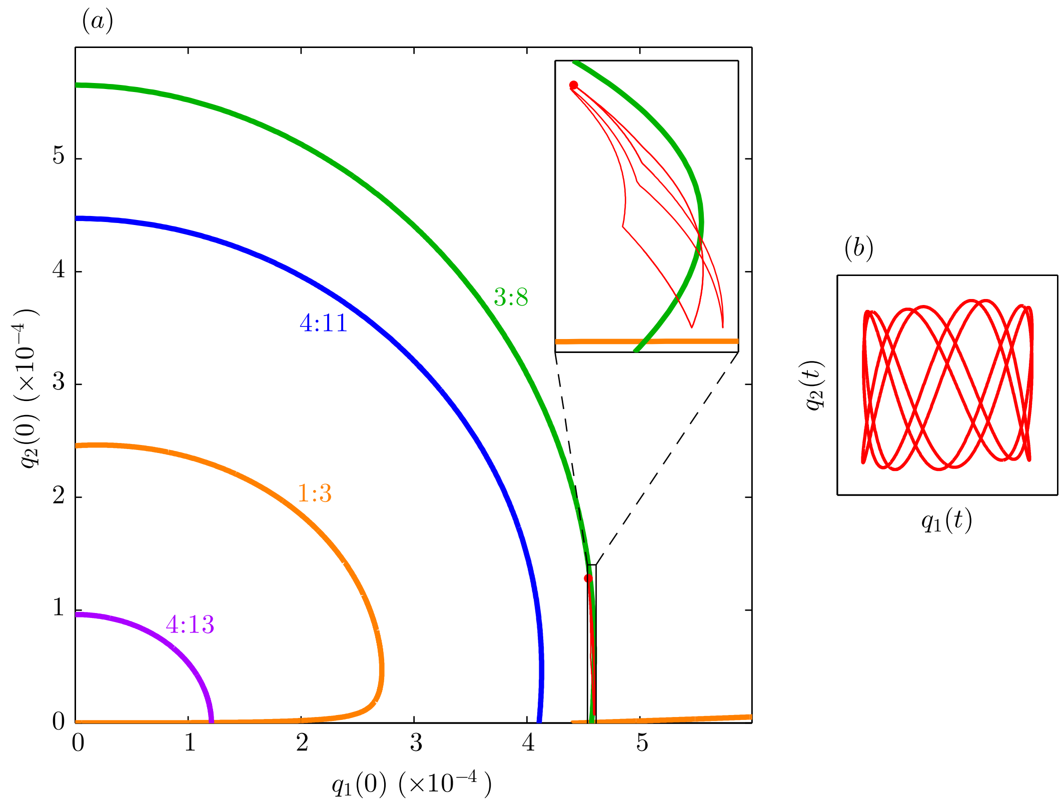

Fig. 4 Panel (a) shows the NNM branches, as given in previous figures, along with a set of forced responses, represented by a thin-red line. A red dot on the forced response branch marks the position of a response that is shown, parameterised in time, in panel (b). The linear modal damping and forcing amplitude are $\zeta = 10^{-8}$ and $F = 0.1$ respectively.

used to show this in detail. A dot on the forced response branch marks the position of a response that is shown, parameterised in time, in Fig. 4(b). This time-parameterised response clearly shows that the forced response also exhibits a 3:8 ratio between the fundamental response frequencies. A comparison may also be drawn with Fig. 2(d), which shows a 3:8 NNM response. It also shows that a slight phase-shift between the modes is present, which allows energy to be transferred between the modes, as discussed in [13].

Conclusions

In this paper it has been shown that the contemporary definition of an NNM encompasses a vast range of possible motions. This has been demonstrated for a simple nonlinear model of pinned-pinned beam with a torsional spring at one end. This leads to a complex picture of the responses, and presents a challenge when using the NNMs to interpret the forced responses of the system. To address this, an energy-based technique was used to investigate the relationship between the NNMs and the forced responses. This revealed that some NNMs require an extremely low damping ratio to relate to a forced response. Such low damping ratios are rarely seen in engineering structures, indicating that these NNMs may be neglected when considering the forced responses of such systems. However, it was also shown that, if the damping is very low, these NNMs may attract the forced responses, and hence they must be considered in these extreme cases.

References

[1] G. Kerschen, M. Peeters, J. C. Golinval, and A. F. Vakakis. Nonlinear normal modes, part I: A useful framework for the structural dynamicist. *Mechanical Systems and Signal Processing*, 23(1):170–194, 2009. Special Issue: Non-linear Structural Dynamics.

[2] A. Cammarano, T. L. Hill, S. A. Neild, and D. J. Wagg. Bifurcations of backbone curves for systems of coupled nonlinear two mass oscillator. *Nonlinear Dynamics*, 77(1–2):311–320, 2014.

[3] T. Detroux, J. Noël, G. Kerschen, and L. N. Virgin. Experimental study of isolated response curves in a two-degree-of-freedom nonlinear system. In *Proceedings of the International Modal Analysis Conference*, 2016.

[4] A. D. Shaw, T. L. Hill, S. A. Neild, and M. I. Friswell. Periodic responses of a structure with 3:1 internal resonance. *Mechanical Systems and Signal Processing*, 81:19–34, 2016.

[5] T. L. Hill, S. A. Neild, and A. Cammarano. An analytical approach for detecting isolated periodic solution branches in weakly nonlinear structures. *Journal of Sound and Vibration*, 379:150–165, 2016.

[6] R. M. Rosenberg. Normal modes of nonlinear dual-mode systems. *Journal of Applied Mechanics*, 27(2):263–268, June 1960.

[7] R. M. Rosenberg. The normal modes of nonlinear n-degree-of-freedom systems. *Journal of Applied Mechanics*, 29(1):7–14, 1962.

[8] S. Shaw and C. Pierre. Non-linear normal modes and invariant manifolds. *Journal of Sound and Vibration*, 150(1):170–173, 1991.

[9] S. Shaw and C. Pierre. Normal modes for non-linear vibratory systems. *Journal of Sound and Vibration*, 164(1):85–124, 1993.

[10] G. Haller and S. Ponsioen. Nonlinear normal modes and spectral submanifolds: existence, uniqueness and use in model reduction. *Nonlinear Dynamics*, pages 1–42, 2016.

[11] T. L. Hill, A. Cammarano, S. A. Neild, and D. J. Wagg. Out-of-unison resonance in weakly nonlinear coupled oscillators. *Proceedings of the Royal Society of London A: Mathematical, Physical and Engineering Sciences*, 471:2173, 2014.

[12] T. L. Hill, S. A. Neild, A. Cammarano, and D. J. Wagg. The influence of phase-locking on internal resonance from a nonlinear normal mode perspective. *Journal of Sound and Vibration*, 379:135–149, 2016.

[13] T. L. Hill, A. Cammarano, S. A. Neild, and D. J. Wagg. Interpreting the forced responses of a two-degree-of-freedom nonlinear oscillator using backbone curves. *Journal of Sound and Vibration*, 349:276–288, 2015.

[14] D. J. Wagg and S. A. Neild. Beams. In *Nonlinear Vibration with Control*, volume 218 of *Solid Mechanics and Its Applications*, pages 261–312. Springer International Publishing, Dordrecht, The Netherlands, 2015.

[15] T. L. Hill. *Modal interactions in nonlinear systems*. PhD thesis, University of Bristol, 2016.

[16] M. Peeters, R. Viguié, G. Sérandour, G. Kerschen, and J.-C. Golinval. Nonlinear normal modes, part II: Toward a practical computation using numerical continuation techniques. *Mechanical Systems and Signal Processing*, 23(1):195–216, 2009. Special Issue: Non-linear Structural Dynamics.

[17] S. A. Neild, A. R. Champneys, D. J. Wagg, T. L. Hill, and A. Cammarano. The use of normal forms for analysing nonlinear mechanical vibrations. *Philosophical Transactions of the Royal Society of London A: Mathematical, Physical and Engineering Sciences*, 373:2051, 2015.

[18] E. J. Doedel, with major contributions from A. R. Champneys, T. F. Fairgrieve, Y. A. Kuznetsov, F. Dercole, B. E. Oldeman, R. C. Paffenroth, B. Sandstede, X. J. Wang, and C. Zhang. *AUTO-07P: Continuation and Bifurcation Software for Ordinary Differential Equations.* Concordia University, Montreal, Canada, 2008. Available at: http://cmvl.cs.concordia.ca/.

[19] T. Hill, A. Cammarano, S. Neild, and D. Wagg. An analytical method for the optimisation of weakly nonlinear systems. *Proceedings of EURODYN 2014*, pages 1981–1988, 2014.